CHAPTER 5

RESULTS AND DISCUSSION

5.1 Dynamics structure of the enzyme at 300 K

5.1.1 Energy minimization

The energy minimization profiles of the apo-enzyme with and without added water molecules have been shown in Figure 5.1.

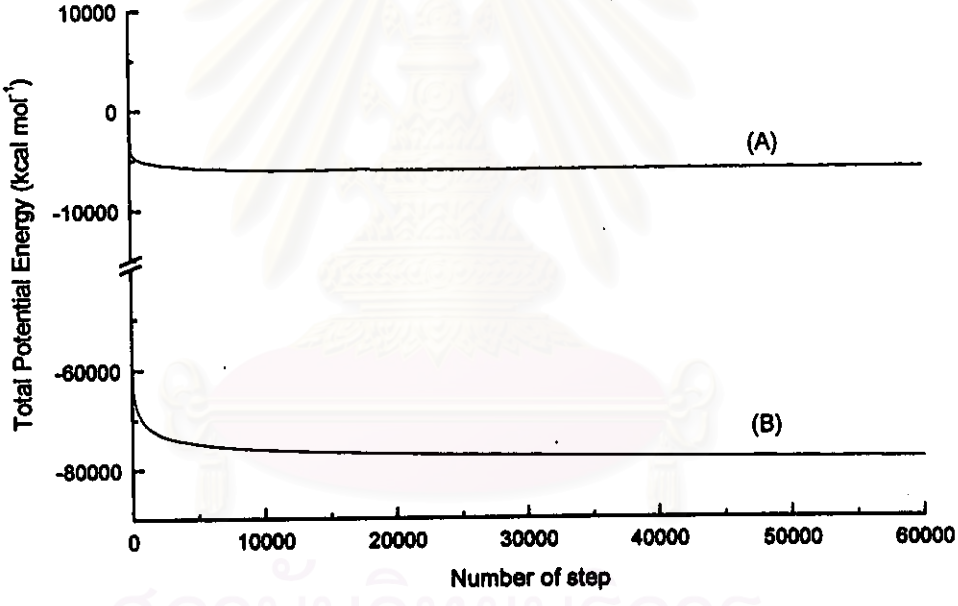

Figure 5.1 A plot of the potential energy of the enzyme (A) in vacuo and (B) in aqueous solution *versus* the iteration steps of energy minimization at 300 K.

As can be seen from Figure 5.1(A), the energy drops rapidly from 4.60×10^3 kcal mol^{-1} to ~ -6.0×10^{-3} kcal mol^{-1} and then stabilized. The final potential energy of the optimized enzyme structure was -6.17×10^3 kcal mol^{-1}. Figure 5.1(b) illustrates the potential energy curve of the apo-enzyme in aqueous solution during the minimization. The potential energy of the system containing the apo-enzyme and water molecules

initiates with -5.33×10^4 kcal mol^{-1} and stabilized to a value of -7.82×10^4 kcal mol^{-1}. The energy profile behaves in similar manner to that of Figure 5.1(A). This suggests that the minimization significantly decrease the strain in the system. The system was gradually relaxed and ready to perform MD simulation for conformational exploration of the enzyme in aqueous solution.

Table 5.1 Potential energy value (initial and final step) of hDHFR during the minimization both in water and vacuum at 300 K.

	Potential energy (kcal mol^{-1})	
	Minimization in vacuum	Minimization in water
Initial value	4.60×10^3	-5.33×10^4
Final value	-6.17×10^{-3}	-7.82×10^4

5.1.2 Molecular dynamics

Figure 5.2 shows a plot of the total energy, kinetic energy, potential energy and temperature of the simulation of the hDHFR calculated over 300 ps. The well-behaved simulation was observed. An initial equilibration occurs rather rapidly and slightly fluctuates over a longer time step. The overall MD profiles obtained were comparable to those observed in other protein simulations[41-43]. Analysis of the dynamics properties was performed after the first 50 ps. The final MD parameters averaged over the last 250 ps were summarized in Table 5.2

(A)

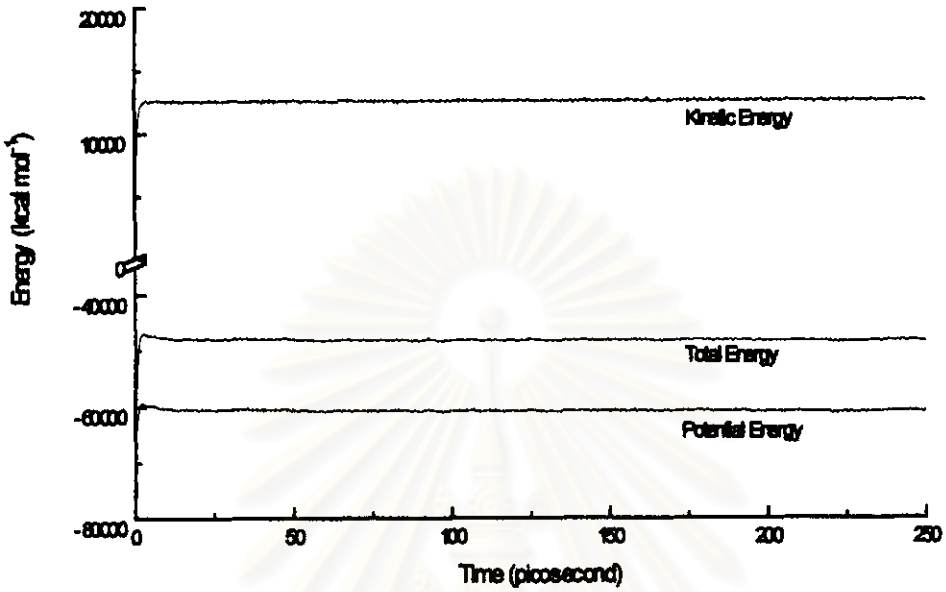

(B)

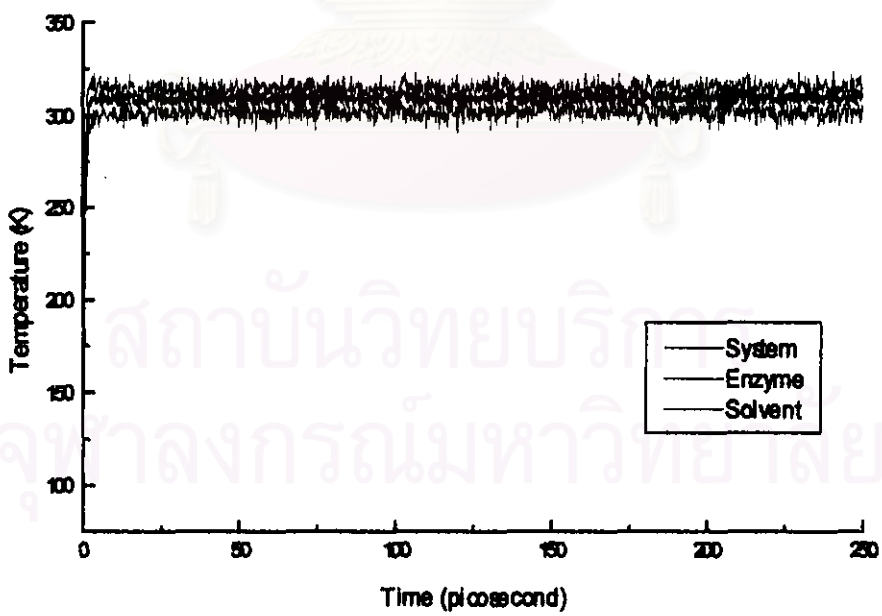

Figure 5.2 MD simulation profiles for the total energy, the potential energy, the kinetic energy (A); and the temperature (B) over the 300 ps of the molecular dynamics simulation for the apo-enzyme-water system at 300 K.

Table 5.2 The final average values calculated from the MD simulation of the apo-enzyme-water system at 300 K.

MD parameters	Mean values
Total energy (kcal $mole^{-1}$) $\times 10^4$	-4.83 ± .009
Kinetic energy (kcal $mole^{-1}$) $\times 10^4$	1.26± .006
Potential energy (kcal $mole^{-1}$) $\times 10^4$	-6.09 ± .011
Temperature of the enzyme (K)	301 ± 4

The MD trajectory and the time-averaged structure

The last 250 ps of the MD trajectory were used to generate an average structure, which was then energy minimized. The time-averaged structure was subsequently used as a reference structure in the calculation of the atomic deviation. The mean global RMSD with respect to the time-averaged one was plotted against the total simulation time of 250 ps (Figure 5.3.).

The distribution of the RMSD for backbone atoms of residues Ser3-Glu183 over the MD trajectory was in a range of 0.50-0.90 Å. Such structural fluctuation is not uncommon in the typical MD simulation of protein, indicating the reliable equilibration of the system in this study. A set of 25 snapshot structures generated every 10 ps out of the 250 ps MD simulation superimposed over each other was shown in Figure 5.3. A superposition of the 25 substructures onto the average structure manifests the mean global RMSD of 1.57 ± 0.17 Å for the backbone atoms and 2.07 ± 0.15 Å for the heavy atoms. As shown in Figures 5.3 and 5.4, the conformations of 25 MD structures superimposed on each other was not significantly different under the time scale of simulation. The segments with large deviation were found to encompass residues Lys80-Gln84 and Pro160-Gly164.

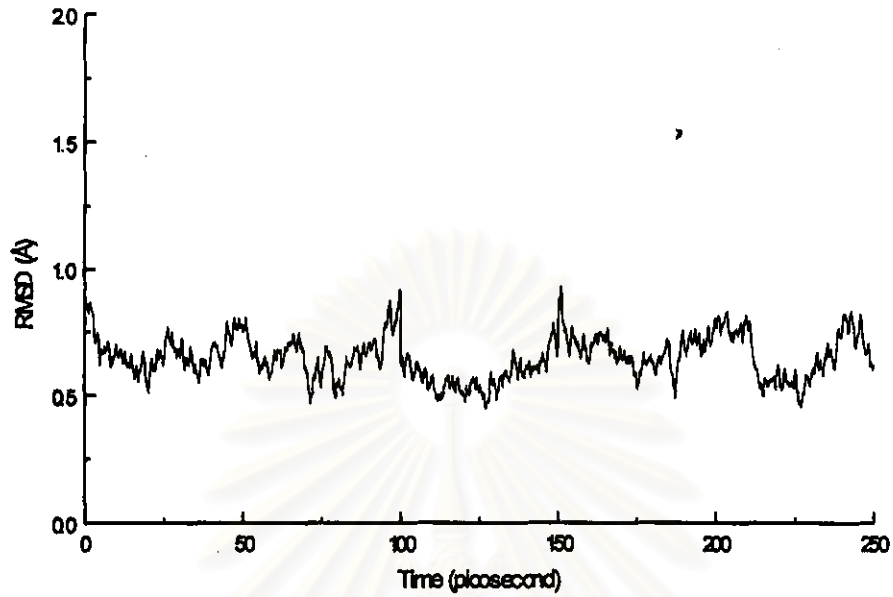

Figure 5.3 **RMSD for the backbone atoms of the human apo-DHFR over the time range of 250 ps. The RMSD values were computed relative to the corresponding backbone atoms of the energy-minimized average structure at 300 K.**

Figure 5.4 **Stereo views showing the Cα-atoms of the human apo-DHFR obtained from a set of snapshots taken every 10 ps through the 250 ps MD simulation at 300 K.**

Apart from the N- and C-terminal, RMSD values for the backbone atoms can be characterized into three categories: little flexible regions (RMSD < 1.0 Å); fairly flexible regions (1.0 Å ≤ RMSD ≤ 2.0 Å); and highly flexible regions (RMSD > 2.0 Å), which correspond to 26.9%, 56.4% and 16.7%, respectively, of a total of 186 amino acid residues. The third category that governs the large conformational changes upon the dynamics simulation time-scale was covered by residues presented in the random coil segments, (Pro25, Pro26, Lys68, Lys80-Gln84, Lys108 and Pro160-Gly164), two α-helical segments αI (Gln35) and αIII (Asp95-Leu97) and two type-turn conformations (Lys18-Asn19 and Asn128-Gly129). The major contribution to an increasing value of the RMSD comes from the solvent-exposed regions. The x–ray structures allow us to locate the amino acid residues within 5.0 Å apart from the folate substrate or its co-factor NADPH . Nevertheless, none of the residues in the third category, except Gln35, was found to occupy a position close to the ligand binding regions.

Solvent accessible surface per residue

The solvent accessible surface area (SASA) was computed using an algorithm developed by Connolly[49]. The mean SASA values of the 25 substructures were higher than that calculated from the crystal structure, suggesting that a slight expansion of the protein volume might occur in some regions of the molecule. This could be attributed to the motion of the side chain as evidenced by the RMSD data (Figure 5.5).

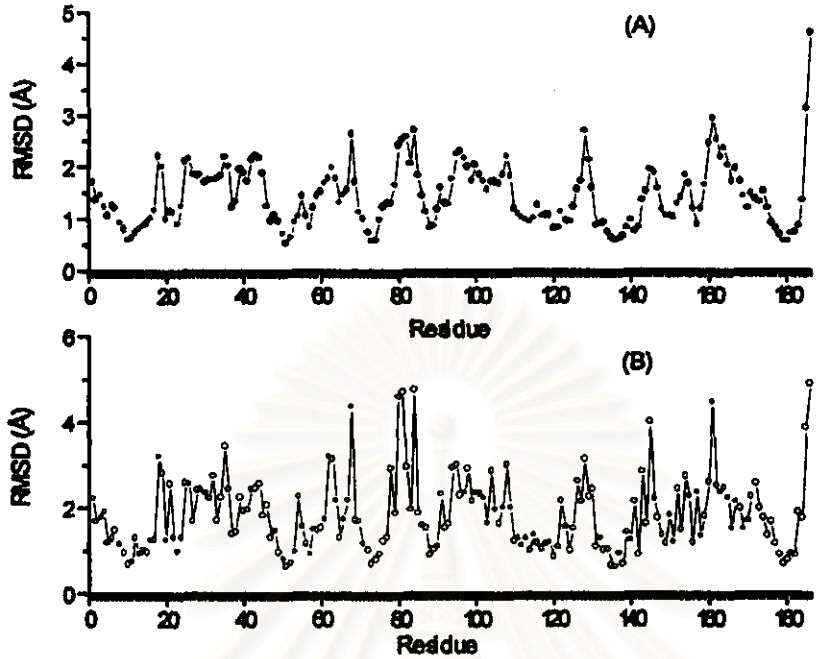

Figure 5.5 A plot of RMSD per residue for the backbone atoms (A) and the heavy atoms (B). The RMSD values were calculated from the 25 MD substructures superimposed onto time-averaged structure at 300 K.

Attempts were made to establish a correlation between the flexibility and the hydrophobicity along the polypeptide segments of the entire protein molecule (Figure 5.6). The observations that the RMSD for all non hydrogen atoms and the SASA values averaged from 25 MD substructures were below 3.50Å and 150Å^2, respectively for over 90% of protein residues implied that the hDHFR might be conformational rigid and hydrophobic. Residues that did not fall into the two criteria were charge and hydrophilicity.

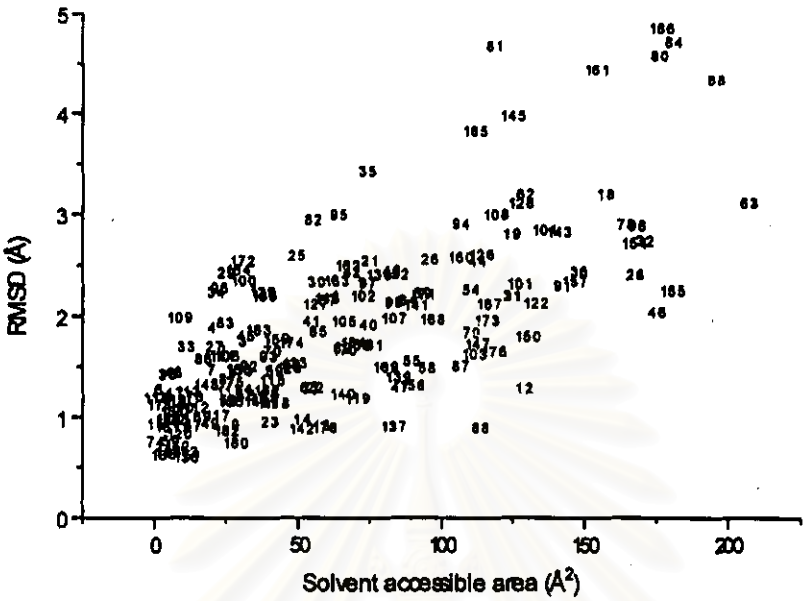

Figure 5.6 A plot of the RMSD of individual residue for the heavy atoms *versus* the mean solvent accessible surface area (SASA). The RMSD values were taken from Figure 5.5. On the graph, the number indicates the protein primary sequence at 300 K.

Although the two criteria (RMSD and SASA values) used seem arbitrarily, our data is in good agreement with the previous structural study of *E. coli* DHFR (ecDHFR). Structural invariance was commonly seen in the vertebrate DHFRs, but not in bacterial DHFRs[44]. In ecDHFR, the strong motion was noted in the segment encompassing Met16-Asn23. In this study, however, the movement of homologous segment Lys18-Pro25 of the hDHFR was found to be notes strong as that observed in ecDHFR. The RMSD values for the heavy atoms of this segment fell between 2.2-3.9 Å. The SASA values calculated from the crystal structure of the ternary complex of ecDHFR were about twofold greater than those of human DHFR apo-enzyme. However, this might not be a sufficiently clear indication to explain the differences of the mobility observed between the mammalian and the bacterial DHFRs. The RMSD and SASA data of residues involving the binding site were given in Table 5.3.

Table 5.3 RMSD and SASA of residues involving the binding site at 300 K.

	RMSD (Å) for		SASA ($Å^2$) from	
Residue	Backbone atoms	heavy atoms	crystal	this work
Ile7	1.21	1.48	9.8	20.1
Ala9	0.80	0.94	22.9	28.4
Trp24	1.23	1.29	20.4	31.1
Glu30	1.70	2.35	19.3	56.4
Phe31	1.75	2.21	108.5	124.7
Phe34	1.83	2.25	45.1	21.3
Thr36	0.56	0.61	74.5	148.2
Thr56	1.06	1.18	26.5	25.6
Phe134	0.73	1.02	9.0	14.1
Thr136	0.56	0.61	2.6	2.0

Assessment of the quality of the protein structure

The 25 MD substructures generated every 10 ps were examined to determine the elements of the protein secondary structure using the algorithm of Kabsch and Sander[45]. The results showed that all residues are in good agreement with Ramachandran diagram (Figure 5.7), except for Ser118. In overall inspection, the backbone dihedral angles, ϕ and ψ, of the apo-enzyme was found to fall within the energetically favored regions, suggesting the good structural quality in this case. Despite the deviations of atomic position and torsion angle, the folding topology and secondary structure elements of the apo-enzyme in solution seem to be identical to those of the enzyme-folate complex in the solid state.

Significant distortions in the secondary structure of the protein molecule were observed for the β-strand segment βD (Phe88-Ser90). Although the strand is structurally conserved among other DHFR's, it completely disappears throughout the entire simulation. This short β-strand might be responsible as the first denatured segment in the unfolding process. Disruption for the α-helical segment (Pro61-Arg65) was also observed

at 65% occurrence during the simulation. However, it is noteworthy that such secondary structure element is not structurally conserved among the known 3D structures of DHFRs.

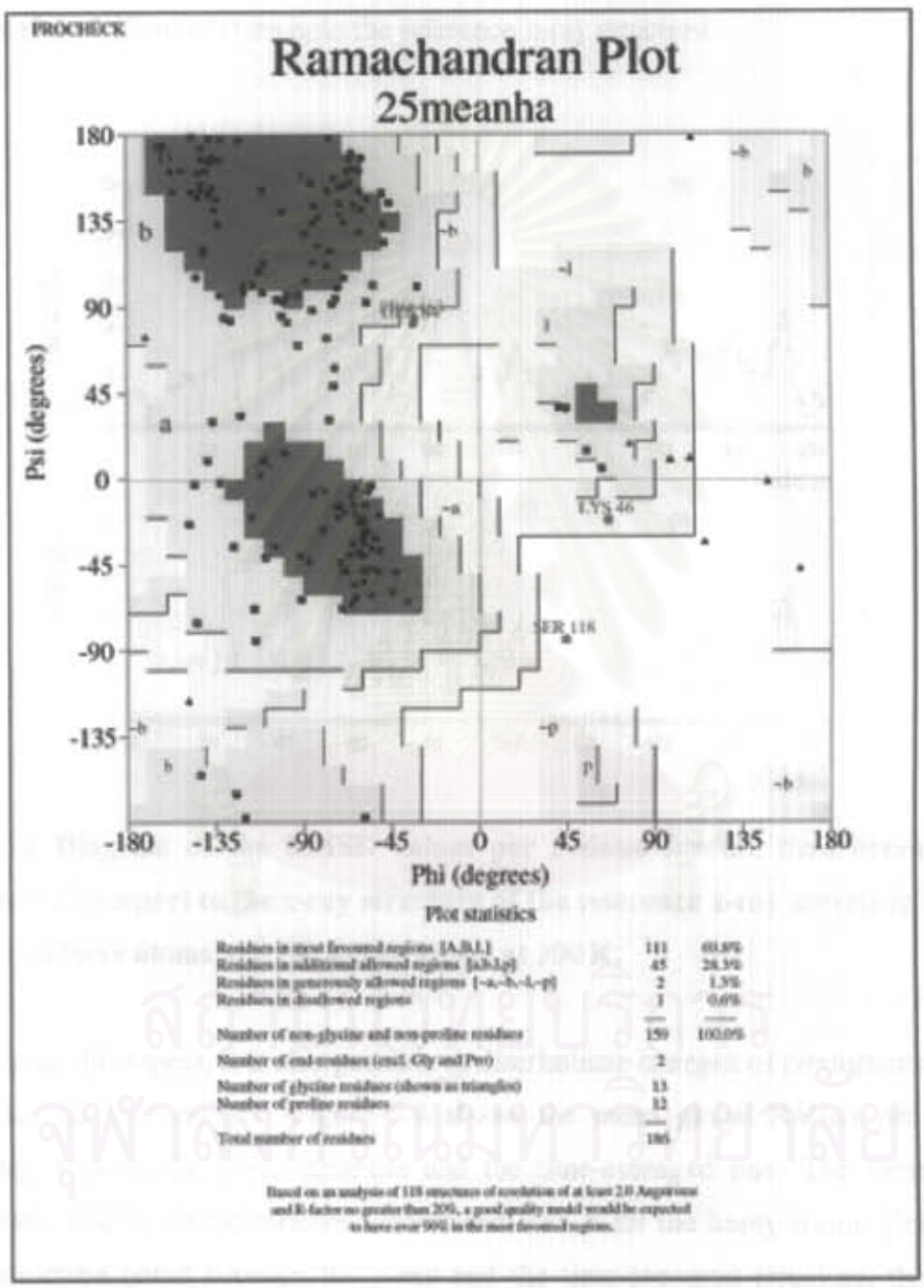

Figure 5.7 Ramachandran plot for the human apo-enzyme produced by the program PROCHECK at 300 K.

Comparison of the x-ray and the time-averaged solution structures

To determine how far the MD structures drifted from the crystal form during the equilibration, structural comparisons were performed by superimposing the mean structure of the MD simulation onto the reference x-ray structure.

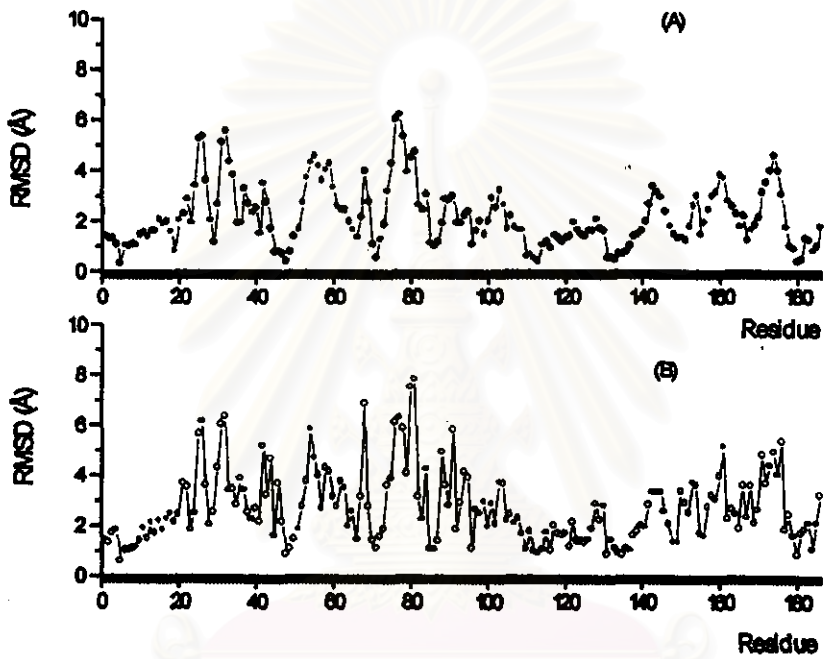

Figure 5.8 Diagram of the RMSD values per residue for the time average MD structure with respect to the x-ray structure of the reference x-ray structure (1DRF) for (A) backbone atoms and (B) heavy atoms at 300 K.

Using this aspect, it is also possible to discriminate changes of conformation upon the bound and free enzyme. Figure 5.8 shows the mean global RMSD per residue comparing between the x-ray structure and the time-averaged one. The mean global RMSD were 2.52 Å for the backbone atoms and 3.15 Å for the heavy atoms. Despite the overall structure noted between the x-ray and the time-averaged structure, there were differences of RMSDs which could reflects some degrees of certain conformational changes as a result of transition from the unbound state of enzyme. The large RMSD differences observed for backbone atoms of Pro25, Pro26, Phe31-Tyr33, Lys54-Thr56,

Ser59, Leu75-Glu78, Lys80, Glu81 and Gly174 accounted for over 4.0 Å deviating from the x-ray hDHFR.

It would be of interesting if the dynamic properties of residues surrounding the active site of this unbound state protein could be determined. To achieve this, amino acids selected from the sequentially conserved residues obtained by homologous alignment between the bacterial (*L. casei*) and vertebrate (human) DHFRs were chosen for the analysis. Our data indicated that, except for Glu30 of which the conformation change was under the mean global RMSD, no significant alteration of protein conformation could be observed from amino acid residues with low RMSD for both the main chain and the side chain atoms.

Deviation of Aromatic rings of phenylalanine side chain

In the case of Phe31 and Phe34 of the wildtype protein, site-directed mutagenesis experiments showed a critical role for the binding efficiency of the ligand in the enzyme catalysis [41]. Investigation of an aromatic ring flipping of the side chain of Phe31 and Phe34 in the absence of ligands might shed some light on the structure/function relationships. As depicted in Figure 5.9., we observed the dynamics information of phenylalanine by monitoring the χ_2 torsion angles of Cα-Cβ-Cγ-Cδ along the MD trajectory signals of Phe58, Phe88, Phe134, Phe142, Phe147, Phe148 and Phe179. The MD data indicated that χ_2 value of most phenylalanine residues were varied between 70°-90° (or equivalent to -110°–90° because of a plane of symmetry in the aromatic ring), except for Phe31 and Phe179 of which the χ_2 values were ~30° or ~ -150°. The average fluctuation of this torsion angle was about ±20°, implying no major rotation of aromatic ring occurring during the simulation time scale.

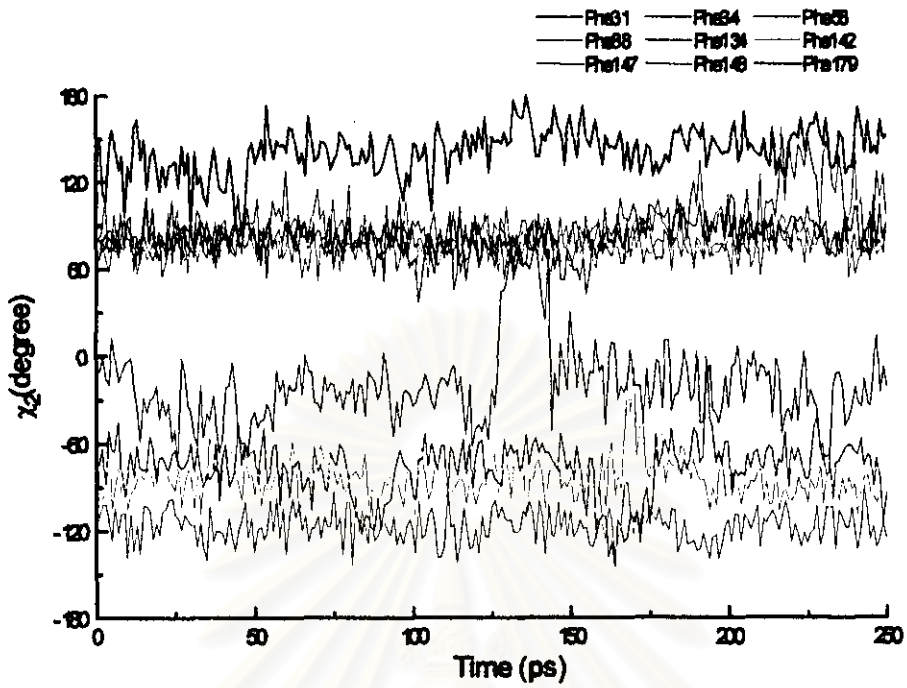

Figure 5.9 Diagrams showing the ring flipping of all phenylalanine presented by the χ_2 fluctuation over the 250 ps of MD simulation at 300 K.

However, an exception was found for Phe31, of which the phenyl ring occupied the largest rotation. As can be seen from Figure 5.9., the flipping could be clearly observed for a time intervention of 30ps beginning the transition at 130ps with the mean χ_2 value of 75° and rapidly returned back to the equilibrium value near 150ps with the χ_2 of -20°. In contrast, χ_2 of Phe34 suggested only a minor movement of the side chain. The differences in orientation and the movement of the side chain between Phe31 and Phe34 in the apo-enzyme were presumable due to the differences in the size of the unoccupied channel(s) around the binding pocket. In the binary and ternary complexes of hDHFR, considerable evidence indicated that the phenyl ring of Phe34 formed a pi-pi stacking with the pteridine ring and the benzene ring of bound folate, but such interaction did not occur in the case of Phe31.

Analysis of the χ_2 of Phe58 revealed that the shift of χ_2 occurred twice: the first transition occurred around 75-100ps while the second transition appeared during 150-175

ps with the mean of intermediate χ_2 of -110°. Such observation should be noted that the unbound enzyme has a low degree of side chain rotation of the phenylalanines.

Comparison of intramolecular hydrogen bonds during the solvation process

It has been well documented that the effect of the interresidue hydrogen bond network plays an important role in folding and stabilizing the protein conformation in aqueous solution. Additional information of the dynamics study of the apo-enzyme could be obtained by identification of the NMR spectra and the MD trajectory in the presence of intramolecular hydrogen bonding in solution. The backbone amide proton was typically used for the characterization of the existence of hydrogen bond in the protein. With the use of slightly different criteria described previously (see legend in Figure 5.10.), the MD results indicated that the 74 amide protons were found to form persistent hydrogen bonds in the apo-enzyme. Nearly 76% of these protons were observed in both free and bound forms of hDHFR. Accordingly, most of these protons having slow exchange with bulk solvent would belong to amino acid residues participating in the regular secondary structures (Figure 5.10A). As previously reported by Stockman *et. al*, sixty six slow exchanging backbone amide protons were identified from homonuclear and heteronuclear NMR spectra of the hDHFR complexed with methotrexate[20]. The number of hydrogen bond observed from our study is comparable to that the binary enzyme-ligand complex. Under the different amide protons, the loss of 15 slowly exchanging amide protons found in the complex enzyme was compensated by the formation of 23 new hydrogen bonds in the apo-enzyme. The amide protons detected from the simulation and from NMR study of the binary complex are summarized in Figure 5.10B. Further analysis of the dynamic structure of the apo-enzyme in solution has led to the investigation of three different types of labile backbone protons according to the frequency of appearance of the hydrogen bonds involved with the labile protons being considered. From a total of 2500 conformations taken from the MD trajectory. Of the total backbone amide (NH) protons, 39.78%, 20.97% and 26.34% could be assigned as persistent, medium and weak hydrogen bonds respectively.

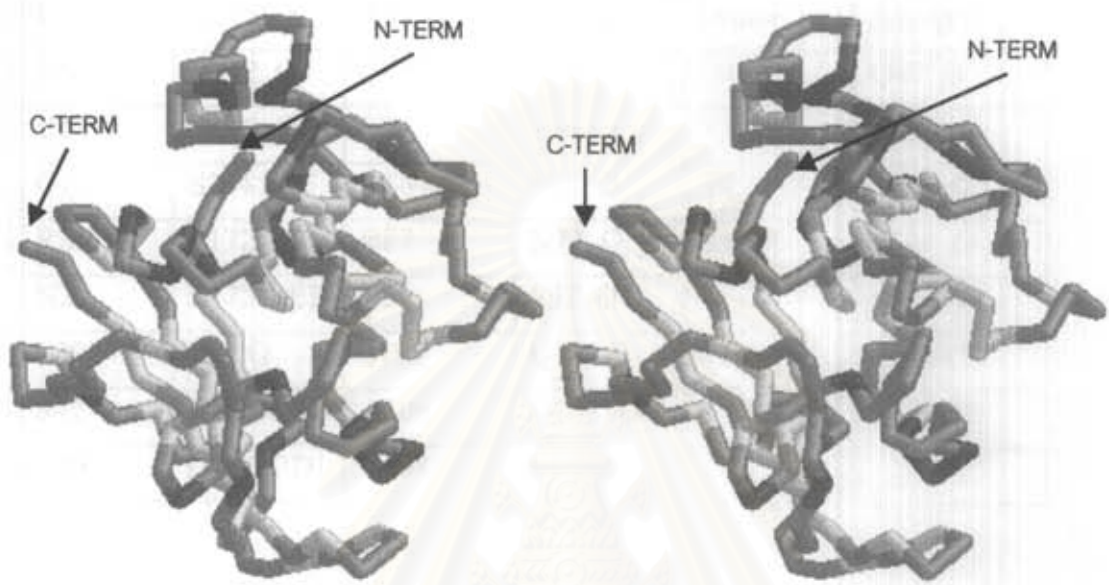

Figure 5.10 (A) Stereo view of the backbone atoms of the energy-minimized average structure of the human apo-enzyme at 300 K. The yellow residues have NH proton exchanging slowly in the enzyme of bound and unbound states; the red ones are observed only in the unbound forms; the green ones are observed in the binary complex and the cyan ones are not observed in both states.

It is interesting to note that the protein segments having either non or weak hydrogen bonds were located on the superficial regions and possessed either the random coil or the turn type conformations. The formation of new hydrogen bonds data is shown in Table 5.4.

Table 5.4 The formation of new hydrogen bonds involving NH backbone protons that were observed in the unbound state enzyme comparing to those from literature [40] at 300 K.

Donor	acceptor	donor	Acceptor	Donor	Acceptor
N5	V112 O	Q47	G45 O	D110	Q47 O
Q12	Q140 O	L79	S76 O	V120	G117 O
G17	S144 OG	A86	P83 O	Y121	S118 O
R28	E172 OE1	H87	N72 O	E123	S119 O
N29	E172 OE2	D95	S92 O	F142	N13 OD1
E30	L27 O	L105	Q102 O	K157	E183 O
S42	D110 OD2	A106	Q102 O	V165	P163 O
V43	D110 OD1	K108	L105 O		

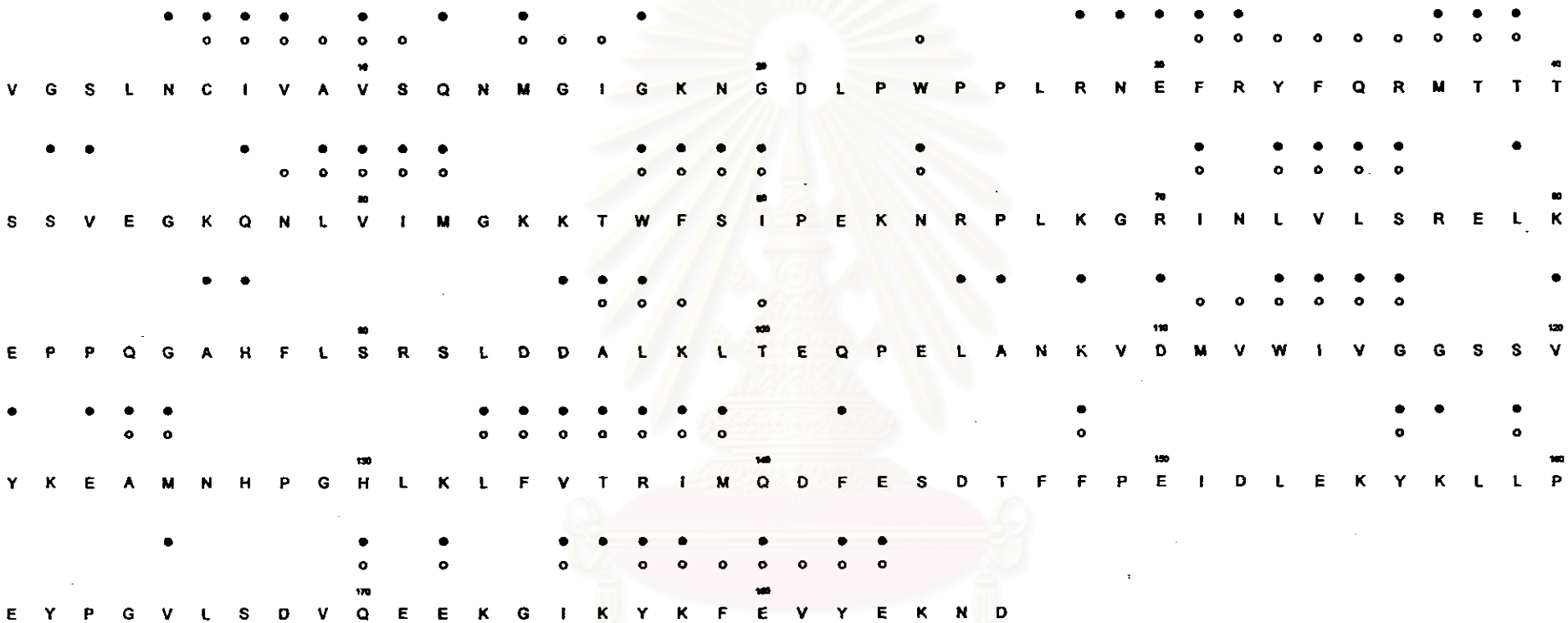

Figure 5.10 (B) **Comparison of residues with slowly exchanging NH protons obtained from the literature (opened circle) and from this study (filled circle), "Persistent", "Medium" and "Weak" hydrogen bonds, those present in more than 90 %, in between 50-90 % and less than 50 % of the conformation along the trajectory, respectively at 300 K.**

5.2 Dynamics structure of the enzyme at 310.5 K

Analysis of the MD simulation at physiological temperature was analogous to that of the 300 K MD. In order to avoid some duplications of the context in the thesis, definition of each MD parameters previously described in Section 5.1 will not be repeated in this Section again. Topics in this section consist of two parts, energy minimization and molecular dynamics. The parameters that were used for carrying out the simulation of the hDHFR in aqueous solution at 300 K were all the same except for the temperature at the thermodynamical equilibration. Relevant parameters and MD properties will be briefly reported as well as discussions of the dynamics structures of the hDHFR at 310.5 K.

5.2.1 Energy minimization

For the energy minimization, the structure of the potential energy profile at 310.5 K is comparable to that of at 300 K as can be seen in Figure 5.11. The energy values at the initial and the terminal energy minimization were summarized in Table 5.5.

Table 5.5 Potential energy value in the initial and terminal steps of the energy minimization both in water and vacuum at 310.5 K.

	Potential energy (kcal mol^{-1})	
	Minimization in vacuum	Minimization in water
Initial value	4.60×10^3	-5.33×10^4
Terminal value	-6.19×10^3	-7.91×10^4

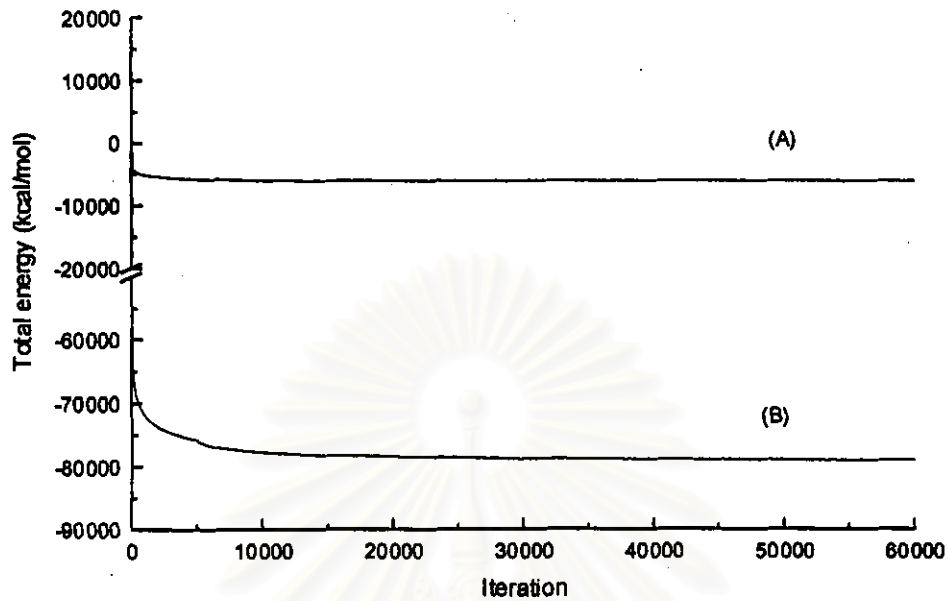

Figure 5.11 A plot of potential energy of the enzyme (A) in vacuo and (B) in aqueous solution versus the iteration steps of energy minimization at 310.5 K

5.2.2 Molecular dynamics

The employment of the MD technique allows us to elucidate structural and dynamics properties of the hDHFR in aqueous solution at physiological temperature. Plots of total energy, kinetic energy, potential energy and temperature along with the simulation time shown in Figure 5.12 illustrate that the equilibration of the system was reached with slight fluctuation. Table 5.6 shows the mean values of the last 250 ps.

(A)

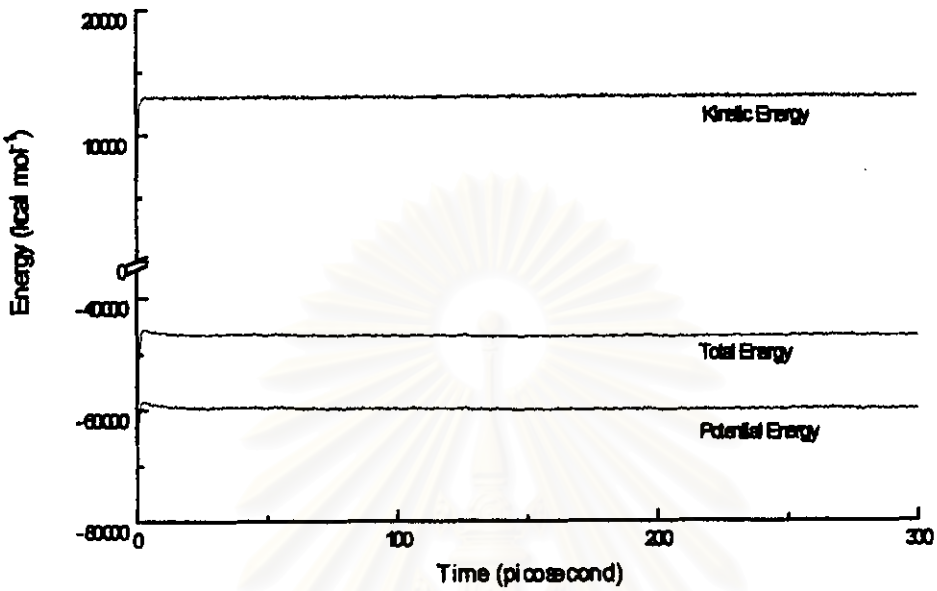

(B)

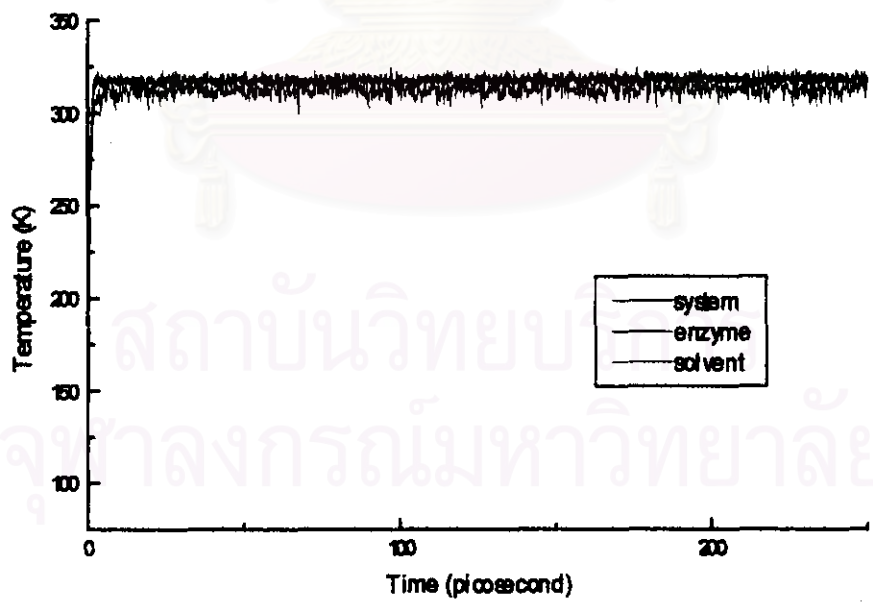

Figure 5.12 MD simulation profiles for (A) the total energy, the potential energy, the kinetic energy; and the temperature (B) over the 300 ps of the molecular dynamics simulation for the apo-enzyme-water system at 310.5 K.

Table 5.6 The final average values calculated from the MD simulation of the apo-enzyme-water system at 310.5 K.

MD parameters	Mean values
Total energy (kcal $mole^{-1}$) $\times 10^4$	-4.69 ± 0.001
Kinetic energy (kcal $mole^{-1}$) $\times 10^4$	1.30 ± 0.007
Potential energy (kcal $mole^{-1}$) $\times 10^4$	-5.99 ± 0.002
Temperature of the enzyme (K)	312 ± 4

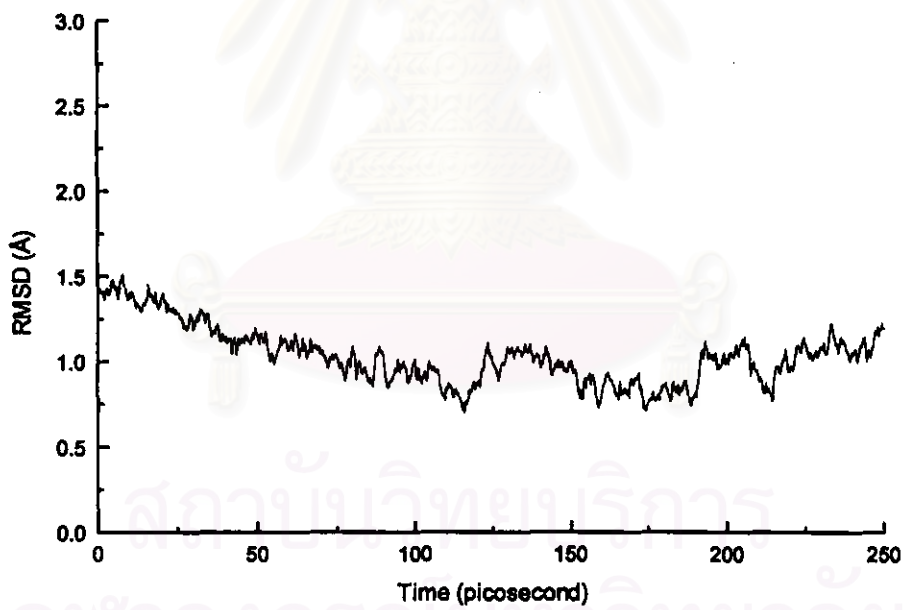

Figure 5.13 RMSD for the backbone atoms of the human apo-dihydrofolate reductase over the time range of 250 ps. The RMSD values were computed relative to the corresponding backbone atoms of the average structure at 310.5 K.

Structural evaluations of the MD trajectory were performed after the first 50 ps. The RMSD for the backbone atoms of residues Ser3-Glu183 fluctuates in a range of 0.75-1.50 Å (Figure 5.13) over the MD trajectory. A set of 25 substructures generated every 10 ps out of the 250 ps MD simulation was shown in Figure 5.14. The mean global RMSD calculated from a superposition of the 25 substructures onto the average one was of 1.53 ± 0.11 Å for the backbone atoms and of 2.06 ± 0.13 Å for the heavy atoms. Figure 5.15 reveals the RMSD per individual amino acid residue of the hDHFR.

Figure 5.14 Stereo views showing the Cα-atoms of the human apo-dihydrofolate reductase obtained from a set of snapshots taken every 10 ps through the 250 ps MD simulation at 310.5 K.

Based on the classification of RMSD values (Section 5.1), 45.7%, 44.1%, and 10.2% out of 186 residues were assigned for less, fairly, and highly flexible regions of this protein, respectively. A plot between the flexibility and the hydrophobicity of the protein depicted in Figure 5.16 illustrates that Lys63, a positively charged residue, is the most solvent exposed (RMSD > 3.50 Å and SASA > 150 $Å^2$). Arg32, Lys46, Lys68, Arg77, Glu78, Lys80, Lys98, Glu101, Lys122 and Lys157 have RMSD < 3.50 Å and SASA > 150 $Å^2$ whereas Asp186, the only one residue, has RMSD > 3.50 Å and SASA < 150 $Å^2$. According to the interpretation of such results, it can be conclude that less than 10% of the protein are highly mobile and hydrophilic.

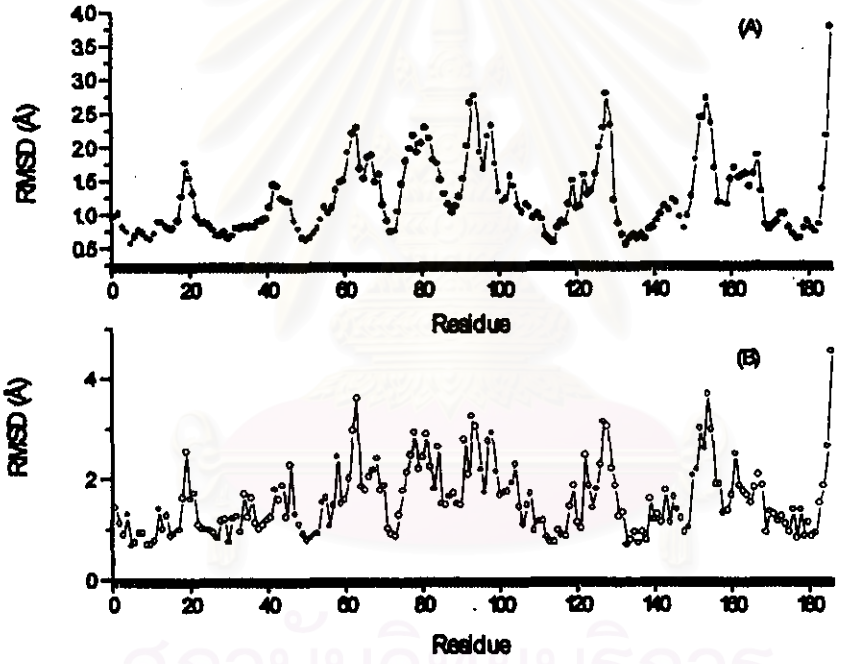

Figure 5.15 A plot of RMSD per residue for the backbone atoms (A) and the heavy atoms (B). The RMSD values were calculated from the 25 MD substructures superimposed onto the time-averaged structure at 310.5 K.

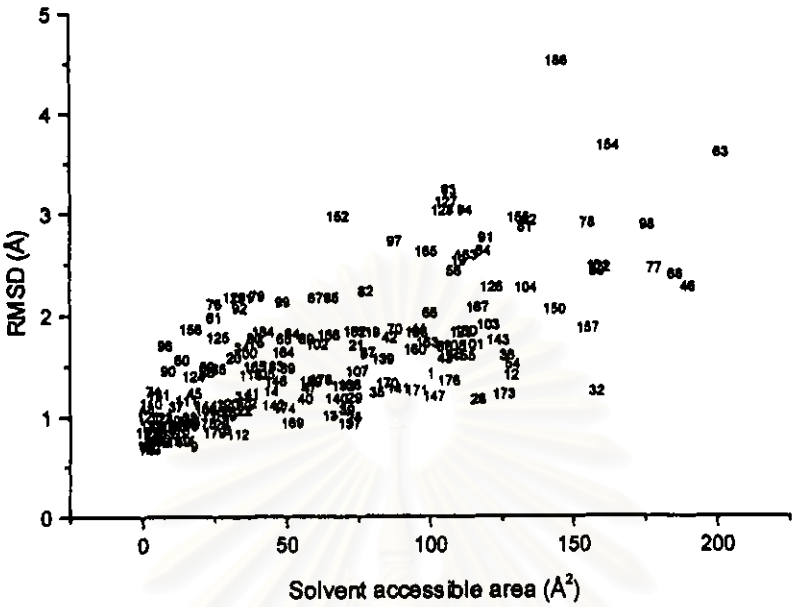

Figure 5.16 A plot of RMSD of individual residue for the heavy atoms *versus* the mean solvent accessible surface areas (SASA). The RMSD values were taken from Figure 5.15. On the graph, the number indicates the protein primary sequence at 310.5 K.

Table 5.7 shows RMSD and SASA of residues involving the binding site.

Table 5.7 RMSD and SASA of residues involving the binding site at 310.5 K.

	RMSD (Å) for		SASA ($Å^2$) from	
Residue	Backbone atoms	heavy atoms	crystal	this work
Ile7	0.76	0.92	9.8	3.6
Ala9	0.66	0.71	22.9	17.7
Trp24	0.87	0.99	20.4	7.8
Glu30	0.65	0.76	19.3	14
Phe31	0.68	1.21	108.5	34.7
Phe34	0.82	1.69	45.1	34.4
Thr36	0.81	1.60	74.5	126.7
Thr56	1.01	1.06	26.5	28.5
Phe134	0.61	0.77	9.0	7.9
Thr136	0.61	0.72	2.6	11.1

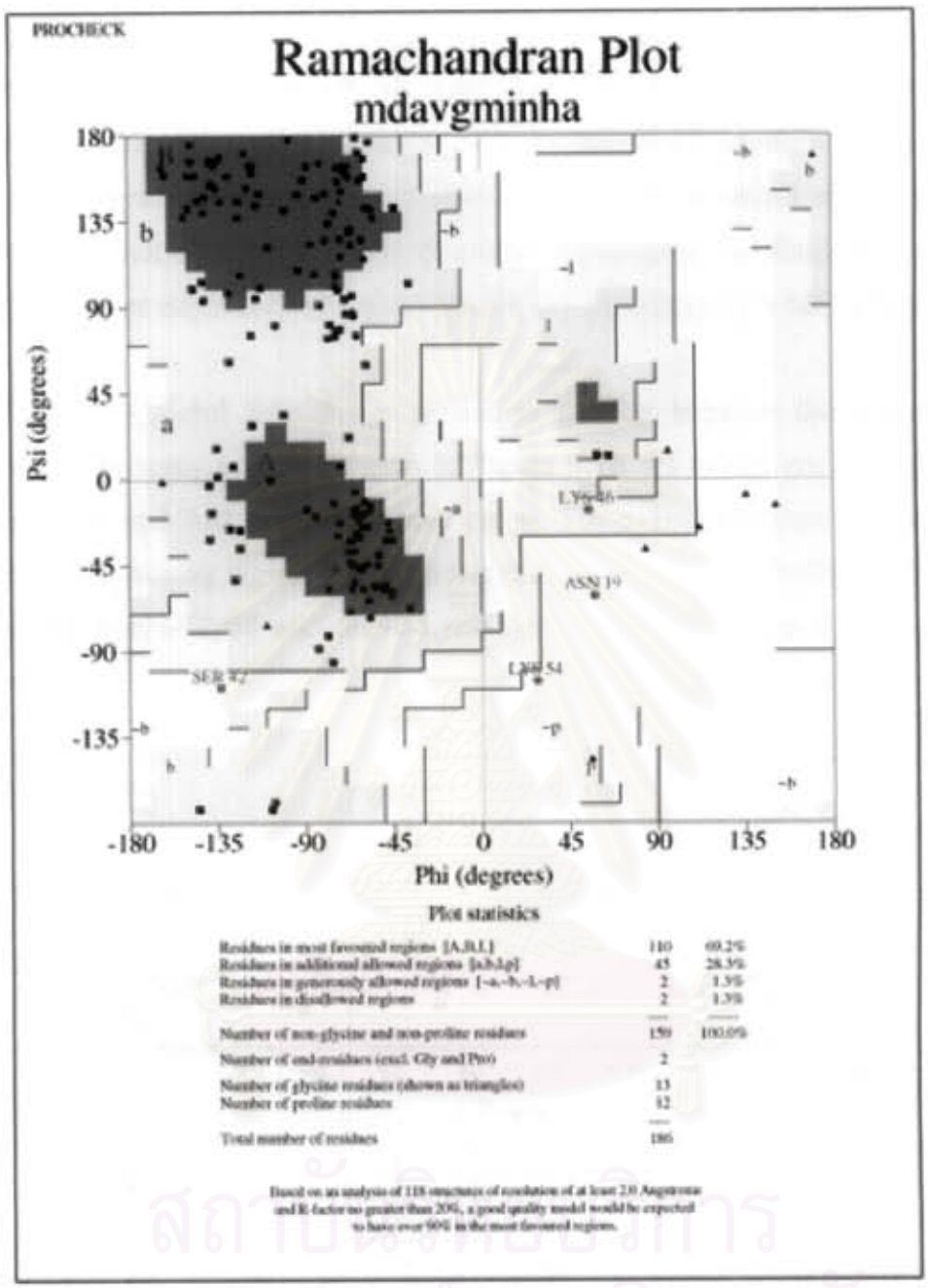

Figure 5.17 Ramachandran plot for the human apo-enzyme produced by the program PROCHECK at 310.5 K.

Ramachandran (Figure 5.17) plot shows the good quality of the main chain structure of the protein except for the Asn19 and Lys54. From an inspection of the secondary structure of the protein in this simulation, the overall structure was identical to that from the crystal structure. Nevertheless, there is one α-helical segment (Pro61-Arg65) that was not observed from the 25 selected structures. The disappearance of the secondary structure might be attributed to insufficient sampling of the MD structure.

The mean global RMSD per residue comparing between the time-averaged structure and the x-ray one was shown in Figure 5.18. Its values are 3.22 Å for the backbone atoms and 3.82 Å for the heavy atoms. The overall structure is quite similar except for the following region, which shows the large deviation, Pro25, Trp57-Arg65, Gly69-Arg70, Ser76-Gly85 and Ser92-Lys98, over 4.0 Å deviation from the crystal structure.

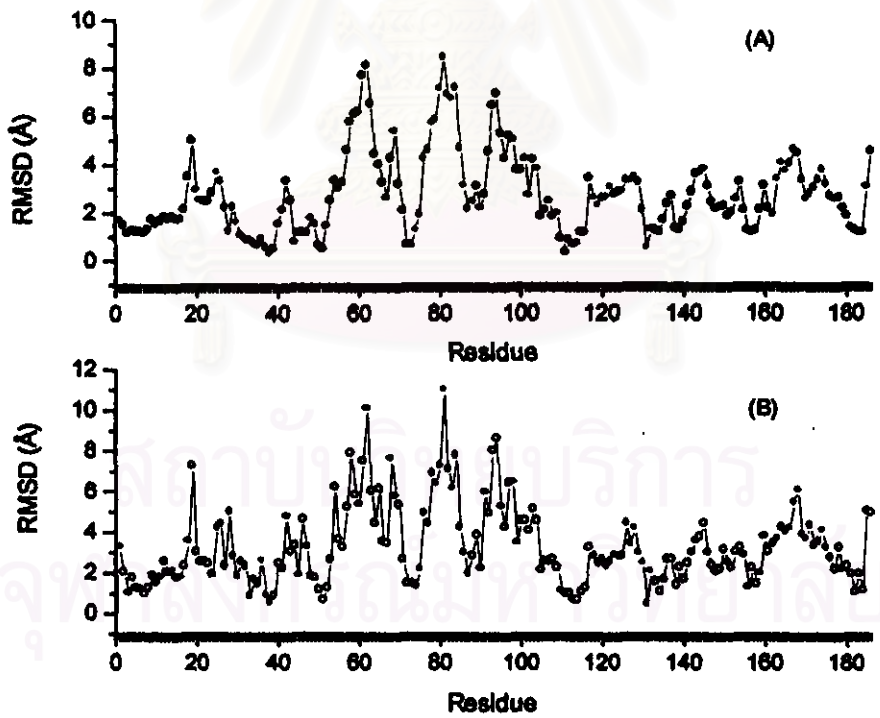

Figure 5.18 Diagram of the RMSD values per residue for the time average MD structure with resoect to the x-ray structure of the reference x-ray structure (1DRF) for (A) backbone atoms and (B) heavy atoms at 310.5 K.

Analogous to the structural analysis of the aromatic rings of phenylalanine side chain from the 300 K MD trajectory, an internal coordinates of Cα-Cβ-Cγ-Cδ, the torsion angle χ_2, were assessed and plotted, giving rise to Figure 5.19. χ_2 values of most phenylalanine residues were approximately 60°-120° (or equivalent to –120°--60°). As can be seen from the Figure, only Phe88 (violet line) shows obviously the aromatic ring flipping. Interestingly, the MD trajectory of χ_2 for this residue consists of two steps of the changing topology. First,. χ_2 changes from ~55° when the simulation undergoes after ~50ps. The first alteration occurs for 20 ps of the time-length and the maximum value of χ_2 was ~15°. Then the second alteration of χ_2 starts immediately, and leads to the flipping of its phenyl ring. for this residue undergoes for primary 65 ps and then permanently flipped after 75 ps.

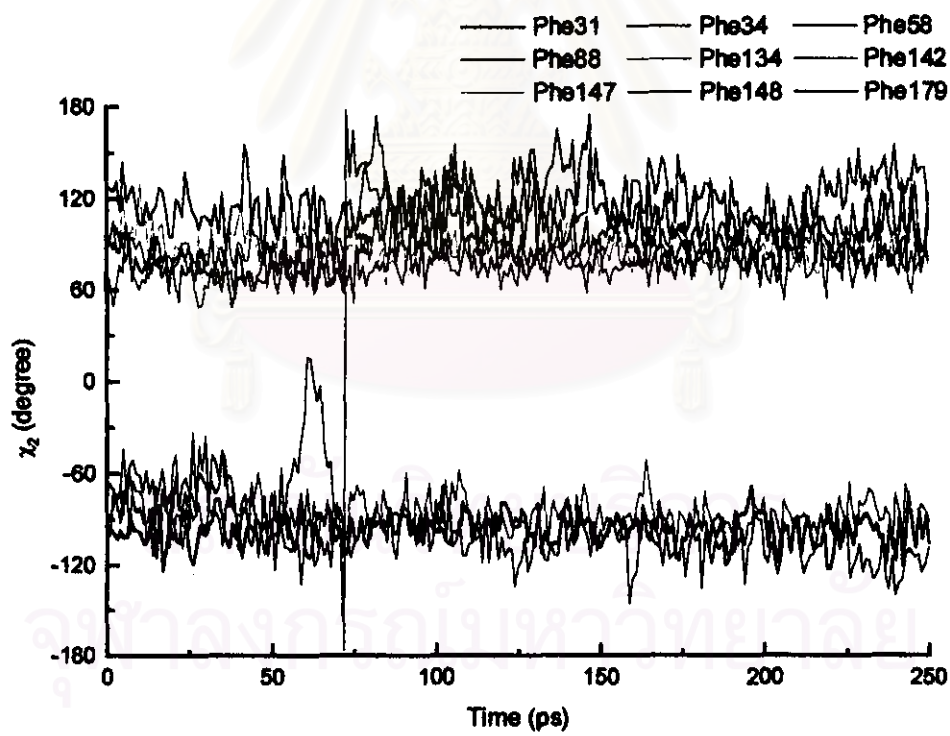

Figure 5.19 Diagrams showing the ring flipping of all phenylalanine presented by the χ_2 fluctuation over the 250 ps of MD simulation at 310.5 K.

Figure 5.20 shows the hydrogen bond that occurred both reported from NMR experiment and MD results. There was 79 amide protons found to form persistent hydrogen bonds in the apo-enzyme. From the previous studied [Stockman et.al.[20]], there were 66 slowly exchanging amide proton found in hDHFR-methotrexate complex. There found 29 new hydrogen bonds forming in the apo-enzyme while 17 hydrogen bonds slowly exchanging amide protons lost during the simulation. The amino acids which participating in hydrogen bond forming both from NMR spectra and MD results were shown in Fig. 5.20A and summarized in Fig. 5.20B.

Taking into the consideration for the frequently appeared hydrogen bonding, they are found the 167 backbone amide proton forming from 2500 conformations. The labile protons considered are categorized into 3 types according to frequently appearance. Those are persistent, medium and weak which are 42.47, 15.05 and 32.26 % respectively. New hydrogen bonds formation is shown in Table 5.8.

Table 5.8 The formation of new hydrogen bonds involving NH backbone protons observed in the unbound state enzyme comparing to those from literature [40] at 310.5 K.

Donor	Acceptor	donor	Acceptor	Donor	Acceptor
S3	D110 O	S90	V74 O	M125	Y121 O
N5	V112 O	D95	S92 O	N126	E123 O
T40	M37 O	L99	A96 O	K132	L4 O
S42	D110 OD2	L105	Q102 O	F142	N13 OD1
K46	D110 OD1	A106	Q102 O	D145	G17 O
Q47	G45 O	K108	L105 O	T146	G17 O
L79	S76 O	V109	A106 O	K155	D152 O
A86	P83 O	D110	Q47 O	V165	Y162 O
H87	N72 O	V120	G117 O	G174	E171 OE1
F88	N72 O	Y121	G117 O	K176	Q140 OE1

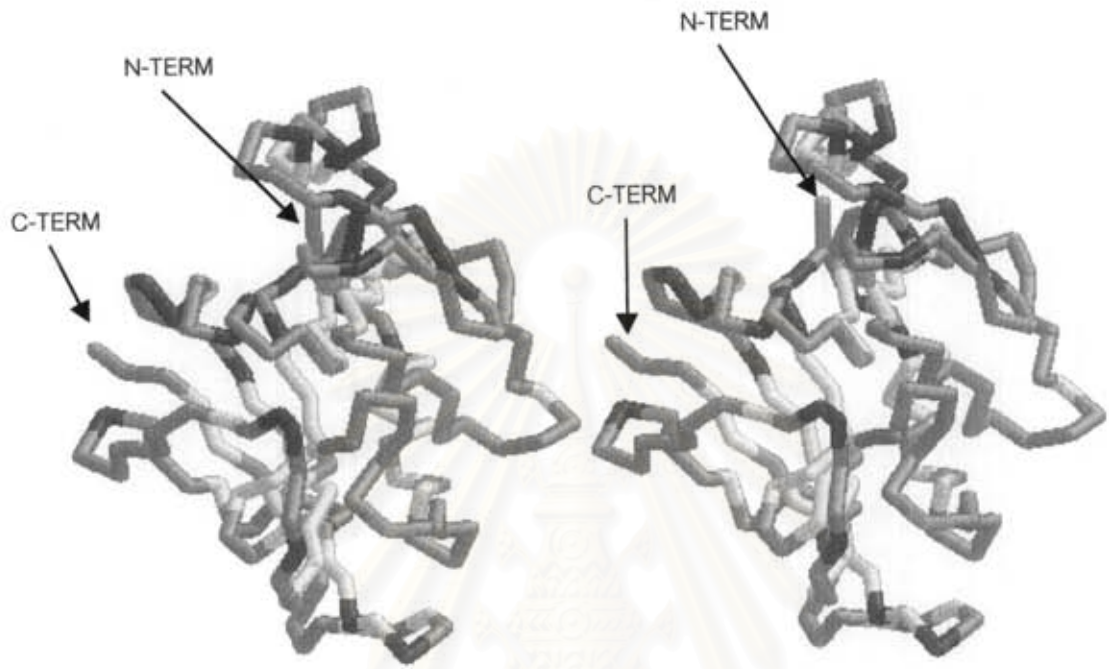

Figure 5.20 (A) Stereo view of the backbone atoms of the energy-minimized average structure of the human apo-enzyme at 310.5 K. The yellow residues have NH proton exchanging slowly in the enzyme of bound and unbound states; the red ones are observed only in the unbound forms; the green ones are observed in the binary complex and the cyan ones are not observed in both states.

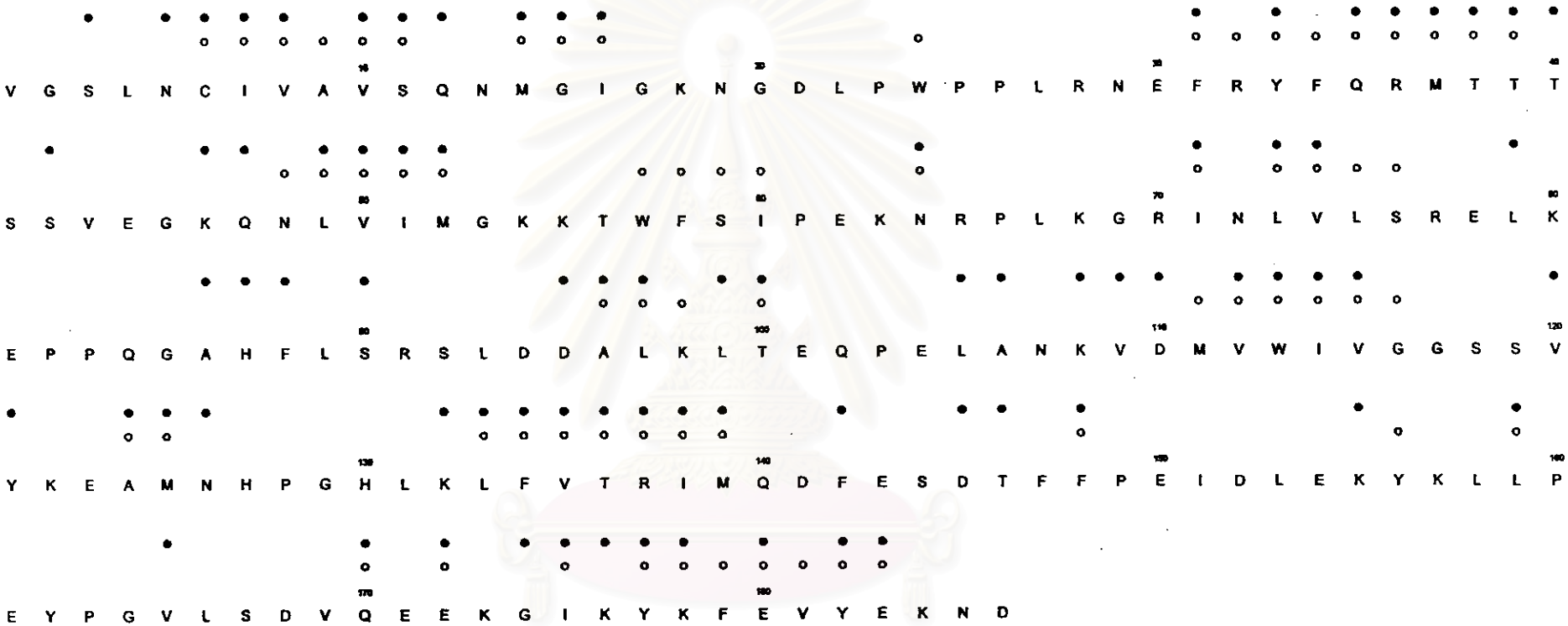

Figure 5.20 (B) Comparison of residues with slowly exchanging NH protons obtained from the literature (opened circle) and from this study (filled circle), "Persistent", "Medium" and "Weak" hydrogen bonds, those present in more than 90 %, in between 50-90 % and less than 50 % of the conformation along the trajectory, respectively at 310.5 K.

5.3 Comparisons of dynamics structures of the two different temperatures

The total energy of the system at 310.5 K is slightly difference from that of 300 K. It increases for 1400 kcal mol^{-1}, this probably due to the increasing of kinetic energy (40 kcal mol^{-1}).

The RMSD along the trajectory of 310.5 K is higher than that of 300 K. This is in general observation that is more fluctuation occurred at high temperature. In contrast, the RMSD within its own family at 300 K is higher but not significant as can be seen from Figure 5.5 and 5.15. The results show different RMSD in the following regions: Pro25-Thr40, Asn107-Asp110, and Leu158-Gly164. The simulated structure at 300 K is quite similar to the crystal one as can be seen from RMSD value (2.52, 3.22 for the system at 300 K and 310.5 K respectively).

The flexibility, which is categorized into 3 regions, shows different result. The flexibility increased from 26.9% to 45.7% in little flexible regions while this value decreased from 56.4% to 44.1% in fairly flexible region and slightly decreased in highly flexible region (16.7% to 10.2%).

The overall solvent accessibility at 2 simulated temperature was not significantly differing. There are some different in SASA and also RMSD values of the residues involving in the binding site as can be seen from Fig. 5.3 and Fig. 5.7.

It was found that in this simulation χ_2 values were similar but not the same as observed in the 300 K simulation. A wider range of the ring flipping might be due to the effect of temperature augmentation. However, dynamics information of the aromatic ring flipping at higher temperature shows some differences with respect to the 300 K MD simulation. There are some differences in χ_2 of Phe31 and Phe88 between the two temperatures as can be seen from Figure X and X. Consider the average structure, we found that side chain of Phe31 at 300 K locate outside the protein. Whereas side chain of this residue at 310.5 K locates inside the protein so it cannot flip. As the same reason, side chain of Phe88 at 310.5 K locates outside the protein while this side chain at 300 K locates inside the protein.

The volume of the 310.5 K system was smaller than that of 300 K. This was made to maintain the pressure to constant value as can be seen from Fig.5.21 and Fig. 5.22.

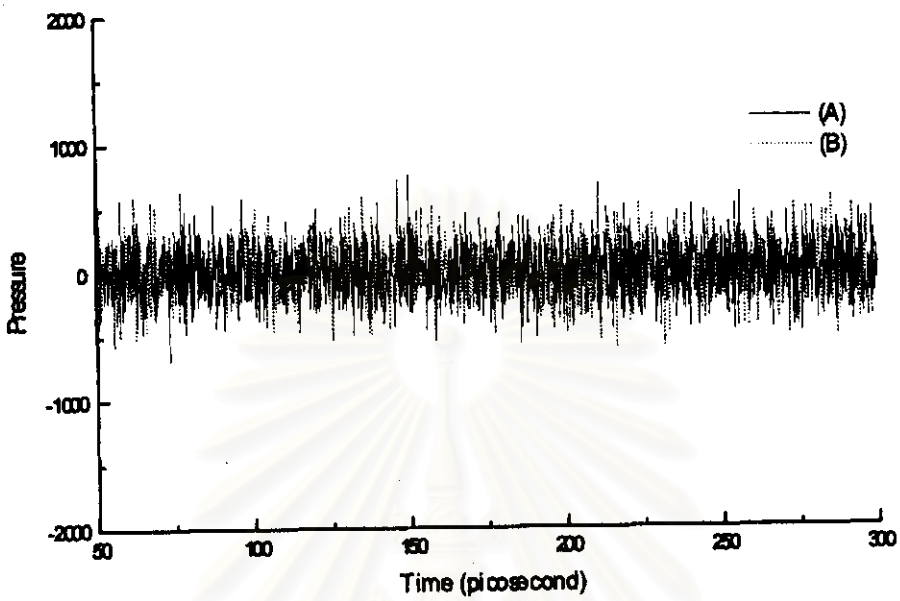

Figure 5.21 Pressure of the system at (A) 300 K and (B) 310.5 K.

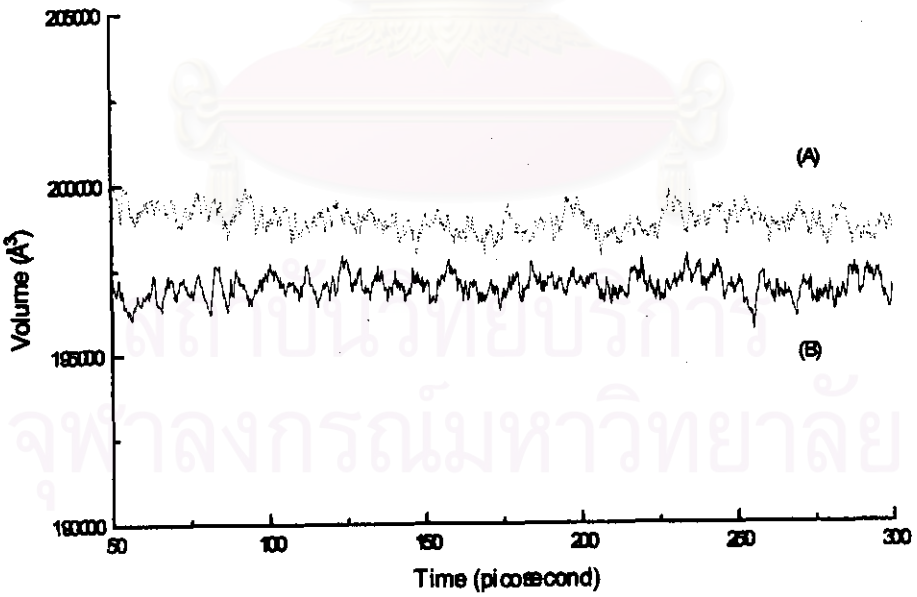

Figure 5.22 Volume of the system (A) 310.5 K and (B) 300 K.

Table 5.9 Comparisons of dynamics structures of the two different temperatures

Properties	**310K**	**310.5 K**
Potential energy (kcal mol^{-1}) of minimization in vacuum		
initial value	4.60×10^3	4.60×10^3
final value	-6.17×10^3	-6.19×10^3
minimization in water		
initial value	-5.33×10^4	-5.33×10^4
final value	-7.82×10^4	-7.91×10^4
Energy (kcal mol^{-1})		
Total energy $\times 10^4$	-4.83 ± 0.0094	-4.69 ± 0.0015
Kinetic energy $\times 10^4$	1.26 ± 0.0065	1.30 ± 0.0066
Potential energy $\times 10^4$	-6.09 ± 0.0011	-5.99 ± 0.0016
Root Mean Square Deviation (Å)		
RMSD along the trajectory	0.50-0.90	0.75-1.50
Global RMSD (superimpose onto the average structure) for backbone atoms	1.57 ± 0.17	1.53 ± 0.11
Global RMSD (superimpose onto the X-ray structure) for backbone atoms	2.52	3.22

Properties	**310K**	**310.5 K**
% Flexibility in little flexible regions (RMSD < 1.0 Å) in fairy flexible regions (1.0 Å ≤ RMSD ≤ 2.0 Å) in highly flexible regions (RMSD > 2.0 Å)	 26.9 56.4 16.7	 45.7 44.1 10.2
SASA of the average minimized structure	11681.71	11326.35
Residue fallen in disallowed region	Ser118	Asn19, Lys54
χ_2 value of Phe side chain	70°-90° (-110°--90°) except for Phe31 (~30°) and Phe179 (~-150°) Note: There is an aromatic flipping of Phe31at 130 ps with the mean value of 75° for a time of 30 ps)	60°-120° (-120°--60°) Note: The flipping occurred at Phe88 for a while at 65 ps with the mean value of 20° and then permanently flipped to 120° at 75 ps.

Properties	**310K**	**310.5 K**
Hydrogen bond		
% Persistent (present > 90%)	39.78	42.47
% Medium (between 50% and 90%)	20.97	15.05
% Weak (less than 50%)	26.34	32.26
Number of Hydrogen bond comparing with the experimental data (NMR)		
Conserving	50 including residue numbers 6,7,8,10,14,31,32,37, 38,39,49,50,51,52,57, 58,59,60,64,71,73,74, 75,76,96,97,113,114, 115,116,124,125,133, 134,135,136,137,138, 139,148,156,159,170, 172,175,177,178,180, 182,183	49 including residue numbers 6,7,8,10,11,14,15,16, 31,33,35,36,37,38,39, 49,50,51,52,64,71,73, 74,96,97,100,112,113, 114,115,124,133,134, 135,136,137,138,139, 148,159,170,172,175, 177,178,180,182,183
New forming	23 including residue numbers 5,12,17,28,29,30,42, 43,47,79,86,87,95, 105,106,108,110,120, 121,123,142,157,165	30 including residue numbers 3,5,40,42,46,47,79,86, 87,88,90,95,99,105, 106,108,109,110,120, 121,125,126,132,142, 145,146,155,165,174, 176

Properties	**310K**	**310.5 K**
Loosing	15 including residue numbers 9,11,15,16,24,33,34, 35,36,48,98,100,111, 112	17 including residue numbers 9,24,32,34,48,57,58, 59,60,75,76,98,111, 116,,156,179,181

Note: The underlined residues refer to the consistency data of the two temperatures.